JOURNAL OF GEOPHYSICAL RESEARCH, VOL. 100, NO. A1, PAGES 251–256, JANUARY 1, 1995

Determination of auroral heat fluxes and thermal ion outflows using a numerical ionospheric model and incoherent-scatter radar data

Q.-L. Min[1] and B. J. Watkins

Geophysical Institute, University of Alaska, Fairbanks

Abstract. A comprehensive one-dimensional model of the polar ionosphere has been used in conjunction with incoherent-scatter radar data from Sondrestrom, Greenland, to determine downward heat fluxes and thermal ion outflows at very high latitudes. For periods of very quiet geomagnetic activity the model closely simulates the observed time-dependent behavior of the electron density, ion and electron temperatures. To obtain this similarity between model and data, the upper boundary conditions of the model, namely downward heat flux, and magnetic field-aligned ion flows, are continually adjusted with time to provide a best fit with data. The heat fluxes and ion flows are determined indirectly from this fitting procedure. The technique has been applied to a 10-hour daytime data set for February 12, 1990, to search for enhanced downward heat fluxes and outward thermal ion fluxes associated with dayside auroral oval. Variations of heat flux ranged from about 2×10^9 to 2×10^{10} eV cm^{-2} s^{-1}, and vertical outward fluxes of ionization ranged from about zero to 8×10^8 cm^{-2} s^{-1}. For both quantities the peak values occurred when the radar site was located under the dayside auroral oval. It is suggested that these marked upward thermal ion flows in the dayside auroral ionosphere may be associated with energetic O^+ ion outflows that have been observed at high altitudes with spacecraft.

Introduction

In this paper we present the comparison of a new one-dimensional ionospheric model with very-high latitude incoherent-scatter radar data. The incoherent-scatter radar located at Sondrestrom, Greenland has been used. The model, originally developed by *Min et al.* [1993] has been further refined by including the effects of neutral winds, and updating the collision frequencies. The unique features of the model is the incorporation of parallel electric fields, the self-consistent computation of the ambipolar electric field, and the effects of time-varying auroral and photoelectron energy distributions. Since the model is one-dimensional, the effects of horizontal transport can not be taken into account, and therefore we have chosen to restrict the data comparisons to periods of quiet geomagnetic activity when horizontal transport is minimal. The altitude coverage of the model used for the data comparison is 100 to 500 km, although the model itself extends to 800 km.

The upper boundary conditions of the model, namely field-aligned thermal ion flow, and downward heat fluxes, are not directly measured with our radar experiments. The model-data fitting procedure is, however, particularly sensitive to these two quantities. We have therefore used this model-data combination to indirectly determine these parameters on a continuous time-varying basis. The model solves the electron transport, continuity, and energy equations, and both ion flow and heat flux values may be determined. The radar-derived temperatures are fitted to the altitude profiles of temperature derived from the model. In the upper ionosphere the magnitude of the total ion composition from the model, and the gradient, is also fitted to the corresponding electron densities and gradients measured by radar.

In the next section the model and method of analysis is presented in more detail.

Model and Method of Analysis

The structure of the thermosphere at high latitudes is significantly affected by solar EUV, and by auroral activity which is caused by precipitating energetic electrons and ions. The solar EUV photons are absorbed in the thermosphere by photoionization and photodissociation, leading to the production of ionization and primary photoelectrons. The primary auroral electrons and/or embedded primary photoelectrons are trans-

[1]Now at Atmospheric Sciences Research Center, SUNY, Albany, New York.

Paper number 94JA02071.
0148-0227/95/94JA-02071$05.00

ported in the atmosphere and produce impact ionization and secondary electrons by ionizing and exciting the neutral species. As a consequence, the temperature and composition of the thermosphere are affected. In turn, the affected atmospheric/ionospheric parameters may perturb the electron transport. A comprehensive one-dimensional self-consistent time-varying auroral model has been developed and used to study the effects of a parallel electric field and the geomagnetic field on the auroral and photoelectron energy distributions, and the response of the ionosphere to auroral precipitations [*Min*, 1993; *Min et al.*, 1993]. In the model the mass spectrometer/incoherent scatter (MSIS) neutral atmosphere is adopted [*Hedin*, 1991], and the electron transport equation, ion continuity equations and electron and ion energy equations are solved self-consistently. This model is described in detail by *Min* [1993] and is only briefly sketched below.

The transit time of auroral and photoelectrons in the thermosphere is short by comparison with changes in the host medium in response to electron impact. Thus the electron transport as well as the energy balance in the thermosphere is considered to be quasi-static. Taking into account elastic and inelastic collisions, the geomagnetic mirror effect, the electric field, the guiding center approximation and conservation of the first adiabatic invariant, and defining the intensity $I(\mathbf{r},\epsilon,\Omega,t) = v^2 f(\mathbf{r},\mathbf{v},t)/m$ [*Duderstadt and Martin*, 1970], the one-dimensional steady state transport equation is

$$\begin{aligned}\mu\frac{\partial I}{\partial s} &- \frac{(1-\mu^2)}{2B}\frac{\partial B}{\partial s}\frac{\partial I}{\partial \mu} - n_e\frac{\partial (LI)}{\partial \epsilon} \\ &- \frac{eE}{2(\epsilon+e\phi)}(1-\mu^2)\frac{\partial I}{\partial \mu} \\ &- \mu eE(\epsilon+e\phi)\frac{\partial}{\partial \epsilon}\frac{I}{(\epsilon+e\phi)} \\ &= -\sum_j n_j {\sigma_j}^{tot} I + Q^{el} + Q^{ex} + Q^{ion} + Q_{photo}\end{aligned} \quad (1)$$

where $I(s,\epsilon,\mu)$ is the electron intensity as a function of the position s, energy ϵ, and cosine pitch angle μ; L is the loss function representing the energy loss to the ambient electrons; E is the electric field related to the potential drop ϕ by $\mathbf{E} = -\nabla 0\phi$, hence $\epsilon = \frac{1}{2}mv^2 + q\phi$, and $q = -e$ for electron; B is geomagnetic field; ${\sigma_j}^{tot}$ is the sum of all loss cross sections; Q^{el}, Q^{ex}, Q^{ion} and Q_{photo} are the sources of elastic collision, excitation, ionization and photoionization, and the summation is taken over all species j. Solving the electron transport equation by adopting and modifying the discrete ordinate method [*Stamnes et al.*, 1988] yields the electron intensity for calculation of the impact ionization and electron heating rates.

To evaluate the ion composition as a function of time and altitude requires solution of the coupled time dependent continuity equations for all reacting species. The continuity equation of species i with density N_i is

$$\frac{\partial N_i}{\partial t} = \eta_d^i + \eta_c^i - N_i L_c^i - \frac{\partial \Phi_i}{\partial z} \quad (2)$$

Here η_d^i and η_c^i are the respective production rates from direct ionization and from chemical reactions. L_c^i is the local chemical and radiative loss rate, and Φ_i is the flux due to ambipolar diffusion and the drift motion resulted from meridional neutral wind through ion-neutral collisions. This flux is computed from

$$\Phi_i = -N_i D_i\left(\frac{1}{N_i}\frac{\partial N_i}{\partial z} + \frac{\partial}{\partial z}\ln T_p + H_i\right) + N_i\omega_D \quad (3)$$

where D_i is the ambipolar diffusion coefficient, T_p is the plasma temperature, and H_i is the plasma scale height. The collision frequencies incorporated in the diffusion coefficients are adopted from *Schunk and Walker* [1970] with the multiplicative factor of 1.7 suggested by *Salah* [1993]. The drift velocity ω_D is

$$\omega_D = -W_M \sin\alpha\cos\alpha \quad (4)$$

where W_M is the meridional neutral wind in the northward direction and α is the dip angle.

We solve the coupled diffusion equations for O^+ and H^+ as the major ions in the F region and above. O_2^+, N_2^+, N^+, and NO^+ are assumed to be in photochemical equilibrium, and therefore we can eliminate the flux divergent term in the continuity equations. In the E region, ionosphere chemical lifetimes are short (a minute or less) which permits this assumption of chemical equilibrium, with diffusion being negligible. Higher in the F region, diffusion is a dominant process and time-scales of an hour or more are required for equilibrium. The time step for our model is 5 minutes. The chemical reactions included here are listed in the work by *Rees* [1989]. Bulk charge neutrality prevails in the ionosphere; having calculated the ion densities, the electron density equates to the sum of all positive ion species.

Several reaction rate coefficients are temperature dependent, requiring the continuity equations to be coupled with the energy equations for the electron and ion gas. Solution of the energy equations yields the electron and ion temperatures. The steady state electron energy equation is

$$\sin^2\alpha\frac{\partial}{\partial z}\left[K^e\frac{\partial T_e}{\partial z}\right] + Q_e - L_e = 0 \quad (5)$$

where K^e is the electron thermal conductivity, Q_e is the electron heating rate, and L_e is the cooling rate. The contribution of the thermoelectric current to the heat flow has been neglected. In the upper F region ionosphere there is substantial exchange of energy between ions and electrons through Coulomb collisions. The ion energy equation

$$Q_{ie} + Q_{E_\perp} - L_{in} = 0 \quad (6)$$

is therefore coupled into the system of equations to be solved. Q_{ie} is the ion heating rate by Coulomb collisions with electrons (an energy loss process for the electron gas), $Q_{E_\perp}$ identifies the joule heating rate, and L_{in} is the ion cooling rate due to elastic and inelastic collisions with neutrals. Conduction in the ion gas is negligibly small and all ions are assigned the same temperature T_i, an adequate assumption for our purpose. Details

and numerical values for all Q and L are given by *Rees* [1989] and *Min* [1993].

There are three groups of coupled equations corresponding to the main physical processes in the thermosphere, which are electron transport, ion diffusion and chemical reaction, and electron and ion energy balance. Simultaneous solution of all the equations is not attempted. Instead, physical arguments are used to simplify the computational problem according to different timescales and altitude regimes [*Min*, 1993]. Those differential equations require boundary conditions appropriate to the physical problem being investigated. For the electron transport equation the lower boundary is assumed to lie within the atmosphere where the density is large, so that the intensity of the electron distribution becomes vanishingly small, while at the upper boundary, we specify the intensity of an assumed electron distribution to fit with data or of a distribution derived from rocket or satellite measurements. For the coupled diffusion equations, photochemical equilibrium prevails at the lower boundary. The O^+ and H^+ fluxes are specified at the upper boundary in order to match the observed profile of electron density. In the meantime, local equilibrium between T_e, T_i, and T_n prevails at the lower boundary for the electron energy equation. A heat flux is appropriate at the upper boundary and is adjusted to match overall the profile of the measured electron temperature from the radar.

The model is one-dimensional and therefore excludes the inclusion of horizontal transport effects. Therefore, we have chosen periods of very quiet geomagnetic activity when horizontal transport is expected to be minimal. Only the component of the meridional neutral wind that is parallel to the geomagnetic field has been taken into account, which forces the ionization up and down at F region heights through ion-neutral collisions and thus changes the height of the F layer peak [*Rishbeth*, 1972]. Therefore, to obtain similarity between model and incoherent-scatter radar data, the meridional neutral wind and the upper boundary conditions of model: namely primary electron distribution, downward heat flux, and field-aligned ion flow, are adjusted to provide a best fit with data.

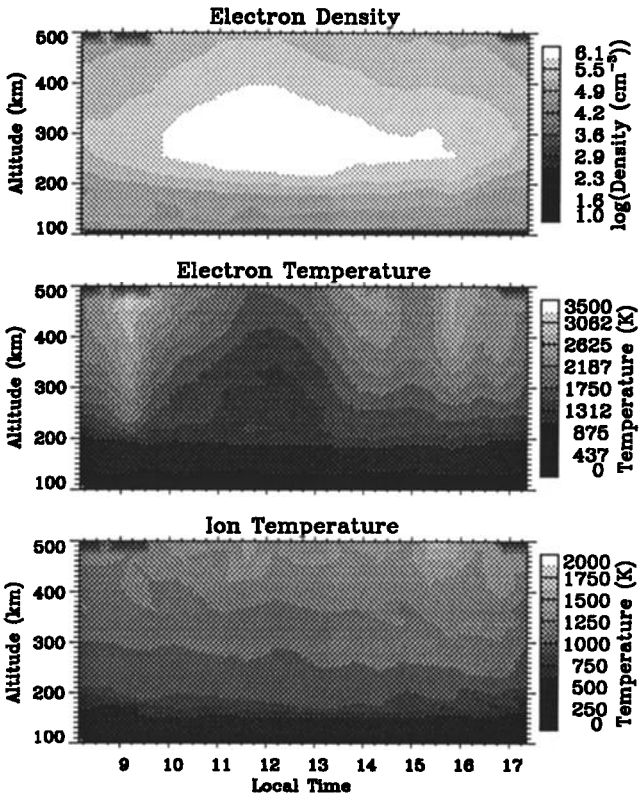

Figure 1. The variation of the electron density, ion and electron temperatures measured over Sondrestrom on February 12, 1990.

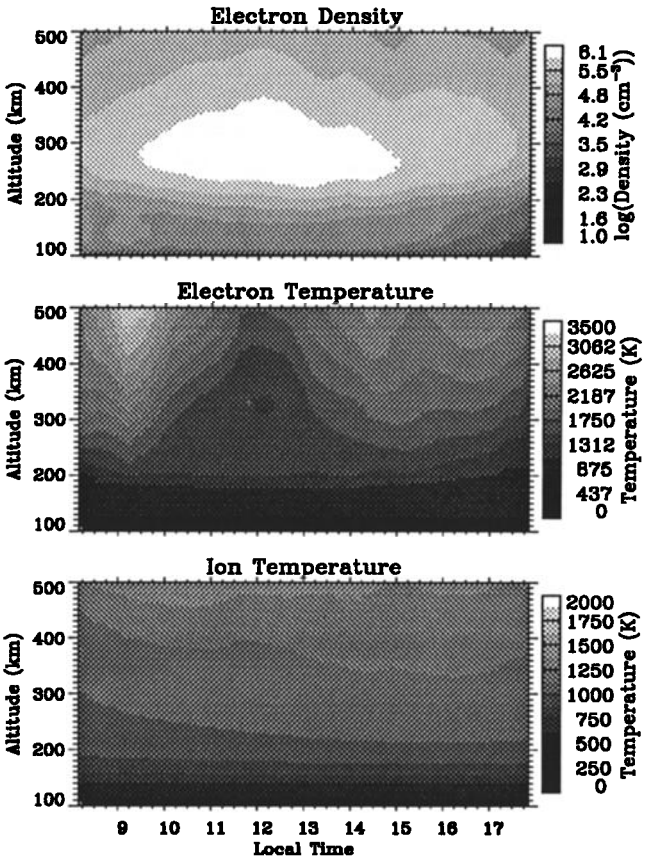

Figure 2. The variation of the electron density, ion and electron temperatures simulated by model over Sondrestrom on February 12, 1990.

Our model covers the region between 100 and 500 km, where the radar signal-to-noise ratio of the measurements is at reasonable level. The outputs of our model, electron density and temperature as well as ion temperature, are nonlinearly dependent on the the meridional neutral wind and the upper boundary conditions of model. In order to simplify the fitting process, we only select a few key parameters to compare with data based on physical arguments. As we know, during typical auroral events, the predominant ionization source for E region altitudes is the auroral electron impact ionization, which allowed us to adjust the auroral electron distribution to fit with data. The height of the F region peak and peak density value, as well as the slope of measured electron density, which represents the overall profile shape of electron density, are deter-

mined by solar EUV and X ray, geocoronal, the meridional neutral wind and field-aligned ion flow at the upper boundary, along with auroral electron precipitation. The electron temperature and its gradient at the upper boundary are primary affected by the electron heat flux from magnetosphere. Therefore we are able to indirectly determine these parameters from incoherent-scatter radar data; this is accomplished by fitting the model to the data; the height of F region peak, F region peak value, the electron temperature, and the slope of measured electron density and temperature in the topside ionosphere, are all fitted with the model by using the steepest descent method [*Press et al.*, 1989]. The time-dependent computation is carried out with a 5-min time step which is much less than the interval of radar measurements (about 15-min). Linear interpolation of the upper boundary conditions is applied to the model time steps between radar measurements.

Results

The variation of the electron density, electron and ion temperatures at various altitudes over Sondrestrom (66.99°N, 309.05°E) on February 12, 1990, have been measured, and a 10-hour sequence of data (0800 LT to 1800 LT) is shown in Figure 1. For this day geomagnetically quiet conditions prevailed (Ap index of 6, and the solar activity index $F_{10.7}$ was 140). We note that just before 0930 LT, the electron density in the E region was even larger than that due to the solar EUV ionization after sunrise, while the electron temperature was enhanced in the F region and above.

The comprehensive ionospheric model is used to simulate the observed time-dependent behavior of the electron density, ion and electron temperatures. The height of F region peak, F region peak value, and the electron temperature and the slope of electron density and temperature at the top altitude from measurements are used as fitting parameters for the model calculations. The EUV flux model of *Tobiska and Barth* [1990] has been used for the solar radiation. However, after the fitting procedure mentioned above, a systematic difference remained between the computed F_2-peak densities and the radar measurements. To achieve the best fit, we have increased the EUV model flux by 50%, which has removed the systematic differences and resulted in the best overall fit. Without auroral precipitation we include a small soft electron flux or photoelectron flux by specifying a downward flux of 0.01 erg cm^{-2} s^{-1} with the characteristic energy of 50 eV as the upper boundary condition for the electron transport equation. As described above, the upper boundary conditions and the meridional neutral wind are adjusted to obtain the similarity between model and data. Comparison of the contours in Figure 1 and 2 shows that the model closely predicts the radar measurements.

The variation of adjusted parameters such as the meridional neutral wind, downward heat flux, and magnetic field-aligned ion flow are shown in Figure 3. The heights of F region peak are well matched between the

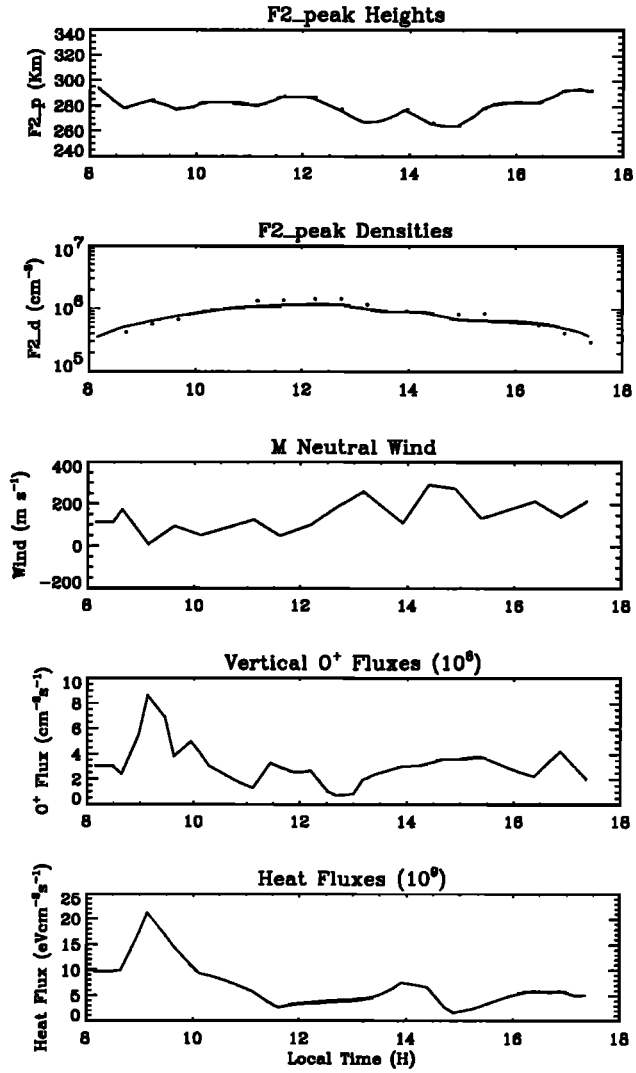

Figure 3. The variation of the F region peak height and density, meridional neutral wind, vertical ion outward flow, and heat flux. The dots represent the measurements, and solid lines represent the model results.

model results (solid line) and measurements (dots) as shown in Figure 3, but the computed densities of the F region peak are smaller than the observations around local noon. The meridional neutral wind increases from sunrise to sunset. The variations of heat flux ranged from about 2×10^9 to 2×10^{10} eV cm^{-2} s^{-1}, and vertical outward fluxes of ionization ranged from about zero to 8×10^8 cm^{-2} s^{-1}. There is a simultaneous enhancement in both downward heat flux and magnetic field-aligned ion flow which correspond to the radar location beneath the dayside auroral oval.

Detailed analysis at three different local times has been conducted by comparing the computed and observed profiles of the electron density, electron and ion temperatures as shown in Figures 4, 5, and 6. These three data sets respectively correspond to times when the radar site is beneath the dayside auroral oval, at the midday density peak, and after sunset. For the first case at 0908 LT (Figure 1) the computed electron density agrees with the measured electron density

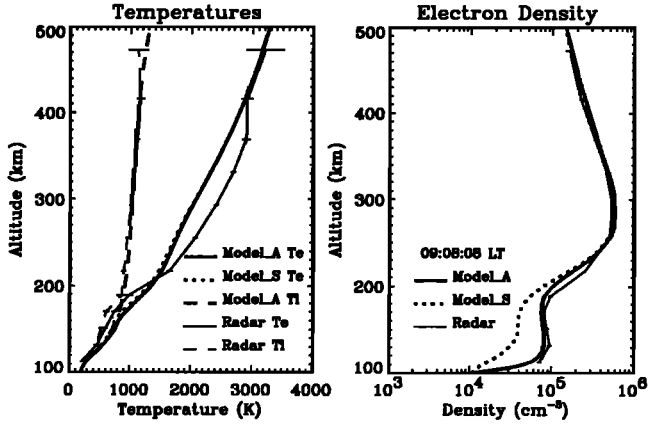

Figure 4. The computed and observed profiles of the electron density, electron and ion temperatures at 0908 LT: the radar measurements (Radar), the model results with solar EUV and auroral precipitation (Model_A), and the model results with only solar EUV (Model_S).

at the F region and above, but the solar EUV input alone is inadequate to explain the observed profiles below 200 km; an auroral precipitation with 750 eV characteristic energy and a 0.5 erg cm^{-2} s^{-1} energy flux has been used to match model results with the observations (see Model_S and Model_A curves in Figure 4). At 1211 LT near local noon the calculated electron and ion temperatures agree with the observed temperatures as well as the overall shape of the electron density profile, however, the magnitude of the calculated electron density is slightly less than the measurements. Figure 6 also shows good agreement between the model results and the radar measurements at 1622 LT, although some differences still exist below 200 km altitude which we attribute to weak time-varying auroral precipitation.

The ion-neutral atomic oxygen collision frequency and the solar EUV flux are crucially important in models of the upper atmosphere and in the derivation of atmospheric results from experimental measurements. Sensitivity tests have been undertaken by varying the ion-neutral collision frequency and the solar EUV flux.

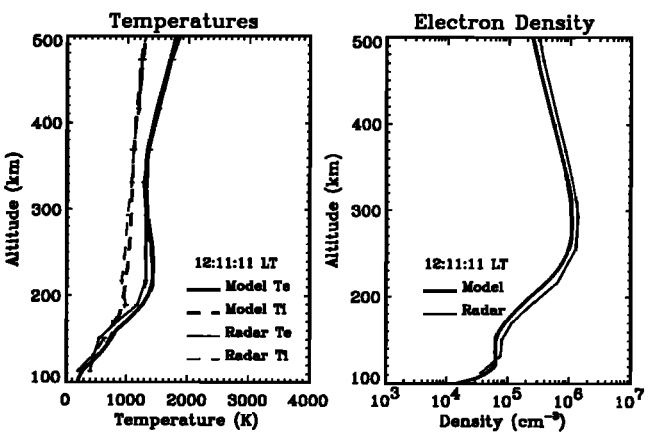

Figure 5. The computed and observed profiles of the electron density, electron and ion temperatures at 1211 LT.

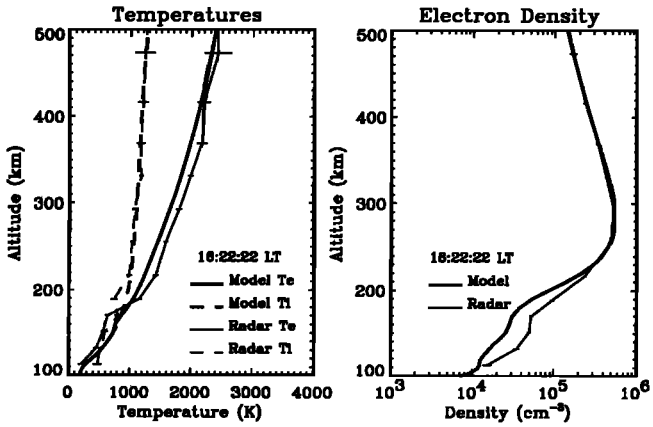

Figure 6. The computed and observed profiles of the electron density, electron and ion temperatures at 1622 LT.

It has been found that a variation of the solar EUV by a factor of 2, results in only about 30% changes in the computed values of the heat flows and ion flows. The main effect of solar EUV flux variation is to change the peak F region density.

The sensitivity test with variation of the collision frequency has shown increases of the heat fluxes and ion flows approximately in direct proportion to decreases of the collision frequency. This follows from (3) where the diffusion coefficient contains the collision frequency. Since collision frequencies in the ionosphere are not well known, we therefore suggest values computed in this paper could be subject to future a revision, however such changes would probably be minor, and the pattern of time variations would remain valid.

Summary

Field-aligned thermal ion fluxes and downward heat fluxes have been indirectly determined. This has been accomplished by using a comprehensive one-dimensional model of the polar ionosphere in conjunction with incoherent-scatter radar data from Sondrestrom, Greenland. The model closely simulates time-varying electron densities and temperatures measured by incoherent-scatter radar. To obtain this similarity, the meridional neutral wind and the upper boundary conditions of the model, viz primary electron distribution, downward heat flux, and field-aligned thermal ion fluxes, are adjusted to provide a best fit with data. Enhanced downward heat fluxes and outward thermal ion fluxes associated with dayside auroral oval have been determined by applying this procedure to a 10 hour daytime data set for February 12, 1990. Variations of heat flux ranged from about 2×10^{9} to 2×10^{10} eV cm^{-2} s^{-1}, and vertical outward fluxes of ionization ranged from about zero to 8×10^{8} cm^{-2} s^{-1}. It is suggested that these marked upward thermal ion flow in the dayside auroral ionosphere may be associated with energetic O^{+} ion outflows that have been observed at high altitudes with spacecraft [e.g., *Yau et al.*, 1984] and future comparisons with spacecraft data may prove valuable. We wish to em-

phasize that the model is one-dimensional and is only applicable to quiet-time data at high latitudes when horizontal transport effects may be ignored. Expansion of this work to three dimensions would permit the inclusion of horizontal transport, and in turn then allow simulation of the disturbed high-latitude ionosphere.

Acknowledgments. This research was supported by the National Science Foundation under grant ATM 9213969.

The Editor thanks A. M. Hamza and N. Singh for their assistance in evaluating this paper.

References

Duderstadt, J. J., and W. R. Martin, *Transport Theory*, John Wiley, New York, 1979.

Hedin, A. E, Extension of the MSIS thermosphere model into the middle and lower atmosphere, *J. Geophys. Res.*, *96*, 1159, 1991.

Min, Q.-L., A self-consistent time varying auroral model, Ph.D. thesis, Univ. of Alaska, Fairbanks, 1993.

Min, Q.-L., D. Lummerzheim, M. H. Rees, and K. Stamnes, Effects of a parallel electric field and the geomagnetic field in the topside ionosphere on auroral and photoelectron energy distributions, *J. Geophys. Res.*, *98*, 19,223, 1993.

Press, W. H., B. P. Flannery, S. A. Teukosky, and W. T. Vetterling, *Numerical Recipes*, Cambridge University Press, New York, 1989.

Rees, M. H., *Physics and Chemistry of the Upper Atmosphere*, Cambridge University Press, New York, 1989.

Rishbeth, H., Thermospheric winds and the *F*-region: A review, *J. Atmos. Terr. Phys.*, *34*, 1, 1972.

Salah, J. E., Interim standard for the ion-neutral atomic oxygen collision frequency, *Geophys. Res. Lett.*, *20*, 1543, 1993.

Schunk, R., and J. C. G. Walker, Thermal diffusion in the F_2 region of the ionosphere, *Planet. Space Sci.*, *18*, 535, 1970.

Stamnes, K., W. J. Wiscombe, S. C. Tsay, and K. Jayaweera, An improved, numerically stable multiple scattering algorithm for discrete-ordinate-method radiative transfer in scattering and emitting layered media, *Appl. Opt.*, *27*, 2502, 1988.

Tobiska, W. K., and C. A. Barth, A solar EUV flux model, *J. Geophys. Res.*, *95*, 8243, 1990.

Yau, A. W., B. A. Whalen, W. K. Perterson, and E. G. Shelley, Distribution of upflowing ionospheric ions in the high-altitudes polar cap and auroral ionosphere, *J. Geophys. Res.*, *89*, 5507, 1984.

Q.-L. Min and B. J. Watkins, Geophysical Institute, University of Alaska, Fairbanks, AK 99775-0800. (e-mail: min@solsun1.asrc.albany.edu; bjw@incoherent.isr.alaska.edu)

(Received May 26, 1994; revised August 8, 1994; accepted August 11, 1994.)